Journal of Crystal Growth 312 (2010) 2564–2568

Contents lists available at ScienceDirect

Journal of Crystal Growth

journal homepage: www.elsevier.com/locate/jcrysgro

Optical probing of low-pressure solution grown GaN crystal properties

J.A. Freitas Jr.[a,*], J.G. Tischler [a], N.Y. Garces [b], B.N. Feigelson [a]

[a] Naval Research Laboratory, Washington, DC 20375, USA
[b] GSNA, Crofton, MD, USA

ARTICLE INFO

Available online 9 April 2010

Keywords:
A1. Characterization
A1. Growth from solution
A1. Impurities
A2. Single crystal growth
B1. Nitrides

ABSTRACT

The structural and optical properties of self-nucleated crystals grown by a near atmospheric pressure solution growth method are presented. High-resolution room temperature Raman scattering studies demonstrate that stress-free crystals with low free-electron background have been produced. Low and room temperature photoluminescence experiments confirm the presence of shallow donors and an unknown shallow acceptor. Large relative intensity variations of the emission bands assigned to recombination process involving donors and acceptor, resulting from significant changes in the incorporation and/or activation of defect associated with each recombination channel, reflect major changes in the intrinsic material properties.

1. Introduction

Despite the lack of high quality native substrates, material research and device development based on heteroepitaxial GaN templates achieved a remarkable progress in early 1990s, after the development of low temperature nucleation layer and p-type conductivity control [1–4]. The increasing interest on III–V nitrides semiconductors was mostly driven by the potential fabrication of optoelectronic devices emitting in the visible/near-UV spectral region. The low quantum efficiency of hetero-epitaxial-based optoelectronic devices was a clear indication of the required use of native substrate to fabricate high quantum efficiency device. The lack of a true bulk substrate and a well established growth technique compelled the material scientists to modify the hydride vapor phase epitaxial (HVPE) growth method introduced by Maruska and Tietjen [5] in late 1960s, to realize the growth of thick/crack-free large area GaN films on sacrificial sapphire substrates. Post-growth processes such as laser-assisted lift-off and chemical etching, and engineered stress releasing interface layers have been developed to realize freestanding substrates up to 3″ diameter [6–8]. These substrates are characterized by dislocation densities typically between middle 10^6 and 10^7 cm^{-2}, and free-carrier concentrations in the middle-low 10^{17} electrons/cm^{-3}. It was demonstrated that homoepitaxial layers with reduced dislocation density and free-carrier concentration could be deposited on these substrates [9,10]. GaN films with lower dislocation densities have been reported on thick films grown by HVPE on sacrificial GaAs substrates using inverted pyramidal pits to enhance dislocations annihilation, but the dislocation densities were rather inhomogeneous across such freestanding substrates [11]. Requirements of homogeneously reduced dislocation density, larger substrate production, and non-polar substrate orientation have motivated the GaN crystal growers to modify vertical HVPE reactors to produce GaN boules of 2″ in diameter and 10 mm in height. This quasi-single crystal boules can be cut to produce basal plane 2″ wafers or a-plane $(1\,1\,\bar{2}\,0)$ and m-plane $(1\,\bar{1}\,0\,0)$ substrates for epitaxial deposition [12]. These polar and non-polar substrates have been successfully used to produce improved quantum efficiency optoelectronic devices [13,14]. The twenty first century commercial needs of higher efficiency solid state lightning and solid state lasers applications require the use of native substrates with lower concentration of extended defects than that achievable by HVPE method. Therefore, it is necessary to pursue research to find new growth techniques capable of growing high quality bulk crystals at high growth rates and low costs. Recently, it was demonstrated that the ammonothermal method, a modified version of the hydrothermal growth technique developed to grow high quality quartz, can be used to grow real bulk GaN substrates which can be sliced on any crystallographic orientation [15,16]. However, the high-pressure and large ammonia volumes, as well as the small growth rate of this method make it expensive for industrial application. Recently, low-temperature and low-pressure methods such as liquid-phase epitaxy based on Na-flux and near atmospheric pressure solution growth processes successfully demonstrated that large area and low-defect concentration crystals could be grown [17,18]. Both the methods are still at developmental stage, but the preliminary results are encouraging.

In the present work, we discuss recent studies of the intrinsic properties of self-nucleated GaN single crystals grown from

* Corresponding author. Tel.: +1 202 404 4536; fax: +1 202 767 1165.
E-mail address: jaime.freitas@nrl.navy.mil (J.A. Freitas Jr.).

0022-0248/$ - see front matter © 2010 Elsevier B.V. All rights reserved.
doi:10.1016/j.jcrysgro.2010.04.013

chemical solution using multi-component solvents, at relatively low pressure and moderate temperature, by means of optical techniques.

2. Sample growth

The GaN samples were grown in a custom-designed growth reactor that is heated by a vertical furnace with multiple elements. The reactor was designed to allow loading of the charged crucible from the bottom and the seed from the top. The developed multi-component solvent, based on Ga–Li melt, utilizes Ga and Li precursors with purity of 99.9999% and 99.9%, respectively, so that any impurity background was unintentional. To prevent oxygen and water contamination the 17 mm inner diameter crucible is charged in a glove-box under nitrogen atmosphere. The polycrystalline GaN source is located at the bottom, while the solvent is located on the top of the GaN source. The position of the crucible in the vertical furnace is selected to introduce an axial thermal gradient in the solution. The reactor is submitted to a sequence of pumping and purging cycles with dry nitrogen gas prior increasing temperature. Growth runs were carried out at nitrogen pressures between 0.23 and 0.25 MPa, and at temperatures of 760–800 °C. The growth runs lasted 50–80 h, and the crucible contents were washed in deionized water and hydrochloric acid to dissolve the remaining products and release the crystals. These transparent and colorless crystals are usually well defined hexagonal shaped platelets with ≤ 2 mm length in the m-direction. Studied crystals were grown in different runs in the solution of same composition. Slight differences in growth temperatures may have caused variations in defects, and impurities incorporation and activation.

The present work focuses on the optical technique studies of self-nucleated crystals to verify the role of impurities and/or native defects in the intrinsic crystal properties.

3. Characterization techniques

Micro-Raman scattering (μ-RS) experiments were performed to evaluate the crystalline quality of the sample and to obtain insights on the free carrier concentration. The measurements were carried out in the backscattering geometry at room temperature. The 1064.1 nm line of a Nd:YAG laser focused down to a 2 μm diameter spot was the probing light source. The sample scattered light was dispersed by a triple spectrometer TRIVISTA 557 equipped with 1200 groves/mm gratings and an OMA V 1024-1.7 liquid nitrogen cooled InGaAs linear-array detector. The instrument spectral band-pass under these conditions was better than 0.15 cm^{-1}.

Room temperature (RT) and low temperature (LT) photoluminescence (PL) measurements were performed to access the optical and electronic properties of the self-nucleated crystals. The low temperature experiments, typically measured at 5 K, were carried out with the samples placed in a continuous helium flow cryostat. The 1.6 K temperatures were achieved by pumping the sample chamber. The room temperature data was obtained with the samples placed in an external *xyz*-translation/tilting stage. The samples were excited with the 325 nm line of a HeCd laser, and the excitation intensity was controlled with UV-calibrated neutral density filters. The sample luminescence, collected and focused with spectrometer f-number matching lenses, was dispersed by a double-grating UV–visible–NIR (near IR) spectrometer fitted with 1800 groves/mm. The spectra were acquired with a UV-extended GaAs photomultiplier tube coupled to a computer-controlled photon counter. Although PL is not a reliable technique to measure the impurity concentration due to simultaneous presence of competing radiative and non-radiative recombination channels, careful comparison with calibrate samples may provide reliable insights on the nature of the dominant recombination channel.

4. Experimental results and discussions

The first order Raman spectrum of a single crystal measured in the $x(zy,zy)\bar{x}$ geometry is represented in Fig. 1. All the allowed phonons in this configuration, namely E_2^1, A_1(TO), E_1(TO), E_2^2 are observed [19]. We also observed the not optically allowed mode E_1(LO) because of light scattering and reflections on the rough side of the crystal. The line shape of the A_1(LO) (observed in the $z(xy,xy)\bar{z}$ geometry, not shown) and E_1(LO) phonons were fitted with a symmetric Lorentzian function (as shown in the inset of Fig. 1 for the E_1(LO) phonon line), which shows that within our experimental error we do not observe electron–phonon coupling effects. At low doping levels (less than 10^{17} cm^{-3}) the linewidth decreases as the background doping decreases and the LO phonons line shape become symmetric. The FWHM reported in this work (see Table 1) are sharper than the ones reported by Bergman et al. [19] indicating that the background doping in this sample is lower than 10^{16} cm^{-3}.

The high-resolution spectrum and the line shape fitting of the sharp E_2^1 (E_2 low) phonon is depicted in Fig. 2. The high-resolution measurements of the full-width-at-half-maximum (FWHM) and the peak position of all the allowed phonons are summarized in Table 1. XRD rocking curves FWHM as low as 16 arcsec have been observed on these samples and they confirm the high crystalline

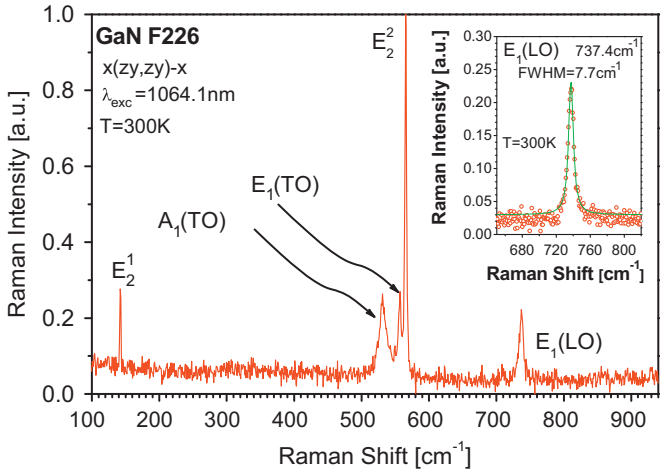

Fig. 1. Room temperature Raman scattering spectrum of a single crystal measured at the $x(zy,zy)\bar{x}$ geometry. The allowed first order phonons are indicated.

Table 1
List of the frequencies and full width at half maximum of the first order phonon observed with the $x(zy,zy)\bar{x}$ backscattering geometry.

Phonon	ω_{ph} (cm^{-1})	FWHM (cm^{-1})
E_2^1	143.0	0.26
A_1(TO)	532.5	13.3
E_1(TO)	557.5	4.7
E_2^2	556.8	3.1
A_1(LO)	733.2	6.9
E_1(LO)	737.4	7.7

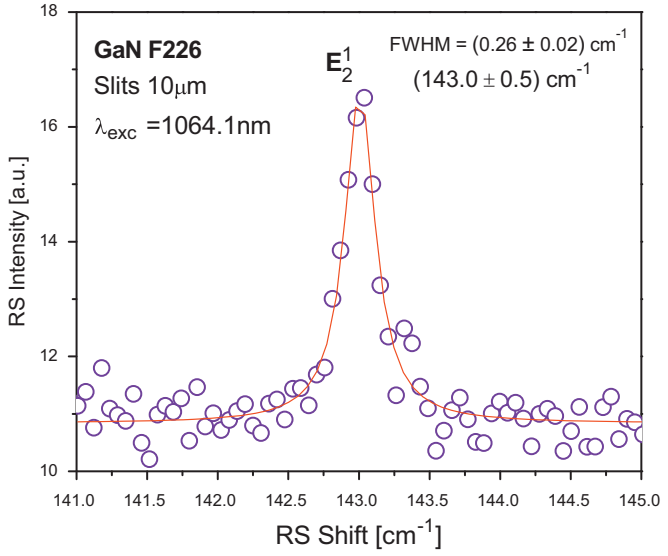

Fig. 2. High resolution Raman scattering spectra, open circles, and best line shape fitting, continuous line, of the E_2^1 low frequency optical phonon.

quality of these crystals [18]. Furthermore, the energy position for the Raman modes is consistent with previous values reported for strain free crystals [19] indicating that these crystals are strain free.

A number of self-nucleated crystals characterized by relatively large spectral intensity variations of various emission bands were selected for this study, to provide a broad overview of the optical properties of crystals grown by this method. Fig. 3 shows the LT and low-resolution PL spectra of four crystals measured in the spectral range between 1.920 and 3.575 eV. All the spectra are dominated by an intense peak near 3.47 eV associated with the annihilation of free excitons and excitons bound to shallow donor and shallow acceptor impurities, commonly called "near band edge" (NBE) emission band, with one LO phonon replica (NBE-1LO) at 3.38 eV. The intense broad band composed of multiple overlapping peaks is assigned to the recombination process involving the annihilation of electrons localized at neutral shallow donors (Si and/or oxygen) with holes localized at presently unknown neutral shallow acceptor, represented by "DAP" (donor acceptor pair) in Fig. 3 [20]. The first peak observed at ~3.27 eV does not involve phonons in the recombination process, and is called non-phonon or zero phonon line (ZPL) DAP recombination band. The additional peaks, shifted toward the low energy side of the ZPL-DAP by multiples of 92 meV, the energy of the A_1(LO) phonon, are called DAP phonon replicas. Also observed in these spectra are the yellow band (at ~2.25 eV, ~551 nm) and the green band (at ~2.37 eV, ~523 nm). While the former are observed in the spectra of samples F226 and H135, the latter is present only in the spectrum of sample C73-1. Yellow and green emission bands have been observed in the luminescence spectra of heteroepitaxial films deposited by different techniques at similar spectral region and they have been assigned to $V_{Ga}O_N$ complexes. However, in the present experiment there is not yet enough experimental evidence to assign these bands to defects with similar chemical structure [21]. The high-resolution PL spectra (acquired with spectral band pass of ~150 μeV) of the NBE emission, between 3.495 and 3.442 eV, depicted in Fig. 4 includes emission lines associated with recombination processes involving the annihilation of free excitons with holes deriving from the valence band A (FX_A) and from the valence band B (FX_B). Also observed, are the intense lines assigned to the annihilation of excitons bound to neutral shallow donors (Si and/or O) leaving the

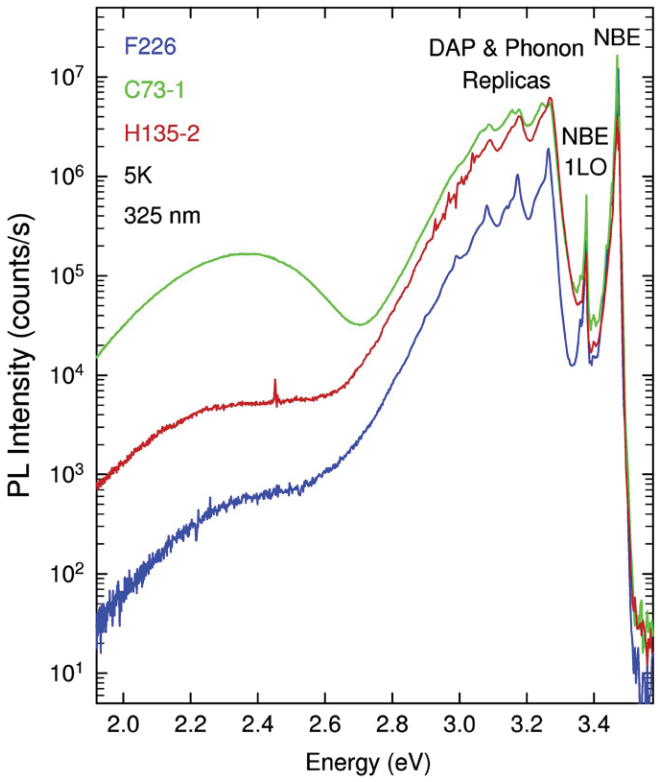

Fig. 3. Low temperature and low resolution PL spectra of three self-nucleated GaN crystals. Changes of relative intensity of the DAP and the NBE emission bands reflects the variation in the concentration of the acceptor and donor impurities.

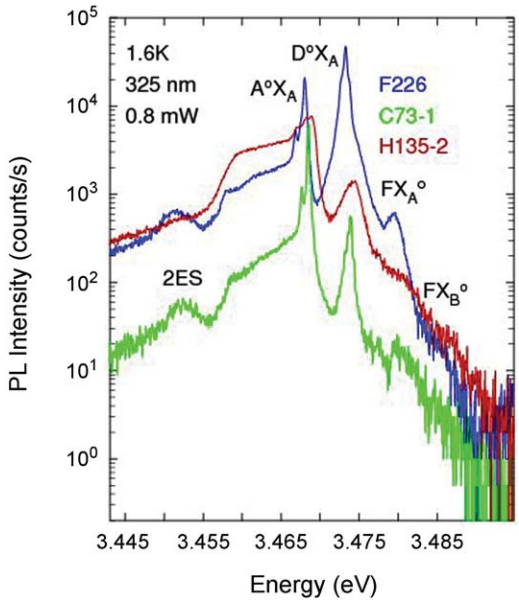

Fig. 4. Low temperature and high resolution spectra of the samples represented in Fig. 3, in the NBE emission spectral region. Note the relative intensity variations of the $D^{\circ}X_A$ and $A^{\circ}X_A$ which are associated with changes in the concentration of donor and acceptor impurities.

donors in the ground states ($D^{\circ}X_A$) at 3.473 eV (FWHM of ~350 μeV, for sample C73-1), and the line related to the annihilation of exciton bound to a neutral unknown shallow acceptor ($A^{\circ}X_A$) at 3.463 (FWHM of ~320 μeV, for sample C73-1) [22]. Note that, upon increasing of the relative intensity of the

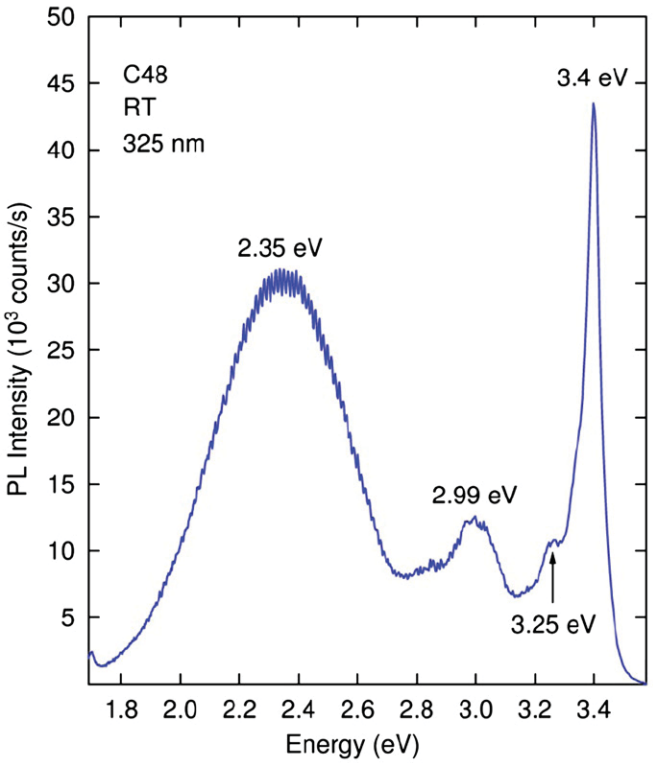

Fig. 5. Room temperature PL spectrum of a self nucleated GaN crystal. The spectrum has similar emission bands observed in films deposited on Sapphire and SiC, which is characterized by relatively low shallow donor concentration.

DAP band highlighted in Fig. 3, the intensity of the FX_A, FX_B, and $D^\circ X_A$ reduce and the line associated with $A^\circ X_A$ broadens and dominates the NBE spectral region. This is consistent with increasing compensation of the shallow donors by increasing incorporation of the unknown shallow acceptors, assuming that the concentration of incorporated donors is constant. It is expected that "at dark" (no photon induced donor neutralization) all donors are compensated, and some of these samples may be at least highly compensated or characterized by high electrical resistivity. $A^\circ X_A$ emission bands with similar energy positions have been observed in Mg and Si doped epitaxial films deposited by MBE and MOCVD on freestanding GaN HVPE substrates [23–25]. Considering the purity of the precursors and crucibles employed in this sample growth method, Mg is not expected as a background impurity. Additional experiments, including mass spectrometry (SIMS), are planned to identify the chemical nature of the shallow acceptor. Note that an unresolved emission line associated with recombination processes leaving the donor in the excited state after the exciton annihilation (two electron satellite or 2ES) is also observed at ~3.45 eV [26]. The observation of sharp exciton related emission lines, which reflects the samples low concentration impurities background, is unusual for bulk GaN samples.

Bulk GaN samples grown from liquid phase equilibrium methods such as high nitrogen pressure and ammonothermal techniques have room temperature free electron concentrations typically between 10^{19} and 10^{20}, which have been attributed to the incorporation of high concentration of oxygen. The low temperature PL spectra of such crystals show a dominant yellow emission band and a weaker and broad and featureless NBE emission band [27,28]. About four orders of magnitude reduction in the free carrier concentration of oxygen in ammonothermal grown crystals was achieved by introducing rare earth with the mineralizer in the autoclave [29]. The low temperature PL spectra of such microcrystalline samples are similar to the spectra observed in the hexagonal platelets discussed in the present work, indicating that the near atmospheric pressure solution growth method produces crystals with relatively low background impurity concentration. Bulk GaN crystals with low background impurity concentration have also been accomplished by Na–Ga melt growth method, as demonstrated by detailed RT Raman spectroscopy and PL studies reported by Skromme et al. [30]. Despite the observation of the $A^\circ X_A$ emission bands with similar energy positions here reported, a dominant deeper acceptor impurity has been assigned to Zn, a well known deep acceptor in GaN.

Room temperature PL measurements were performed at low excitation conditions on selected as-grown samples to verify the dominant recombination process, in the attempt to obtain insights on the electronic properties of these unintentionally doped (UID) crystals, by comparing these results with well characterized epitaxial films. Fig. 5 shows the low resolution RT PL spectrum of a crystal, which is dominated by a relatively sharp emission line at 3.4 eV and a broad green-yellow emission band at 2.35 eV. The 3.4 eV emission results from the overlapping of contributions from recombination processes involving electrons in the conduction band and holes from the valence bands (band-to-band), since at RT the majority of the shallow donors transfer their electrons to the bottom of the conduction band due to thermo-ionization, and recombination processes involving free-exciton with holes from the A, B, and C valence bands. Also observed is the weak ~3.25 eV band associated with recombination process involving electrons in the conduction band with holes bound to an acceptor (free-to-bound or F–B) and the unknown near-UV band at ~3.0 eV. Emission bands with similar energy to the latter band are frequently observed in UID high-resistivity films grown by MOCVD technique [31]. Emission bands near to this spectral position have also been reported in PL studies of films intentionally doped with carbon to generate high resistivity films [32]. Higher resolution RT PL spectrum of the NBE spectral region of the sample yields FWHM in the order of 35 meV, which is a relatively small value compared with reported values for bulk crystals [16]. Previous PL and transport results, reported on UID and Si-doped GaN films deposited on sapphire and SiC, indicate that the spectra represented in Fig. 5 are consistent with the samples with an excess of uncompensated shallow donors, which are the source of electrons in the conduction band responsible for RT n-type conductivity [33]. Preliminary electron paramagnetic resonance measurement carried out on similar sample yield a background donor concentration of middle $10^{15}\,cm^{-3}$. This value is close to that observed in micro-crystals synthesized by ammonothermal method employing oxygen rare earth getters [29].

Samples with different relative intensities of recombination processes associated with donors and unknown acceptors have also been produced and studied. Fig. 6 depicts the RT PL spectra of two additional UID self-nucleated crystals. The samples have been measured at lower excitation condition to minimize heating and photo-neutralization of the charged donors, which will increase the intensity of the NBE emission band. Note that the lower intensity spectrum acquired for Sample C85B, which has been multiplied by 3, has all the emission bands observed in the spectrum of Sample C48 (Fig. 5), with exception of the ~3.0 eV emission band. The intensity of the NBE emission band in this spectrum is reduced, as compared with that in Fig. 5, while the intensity of the DAP is relatively larger. This is consistent with increasing acceptor concentrations, assuming similar background concentrations of shallow donors. The spectrum of Sample H135

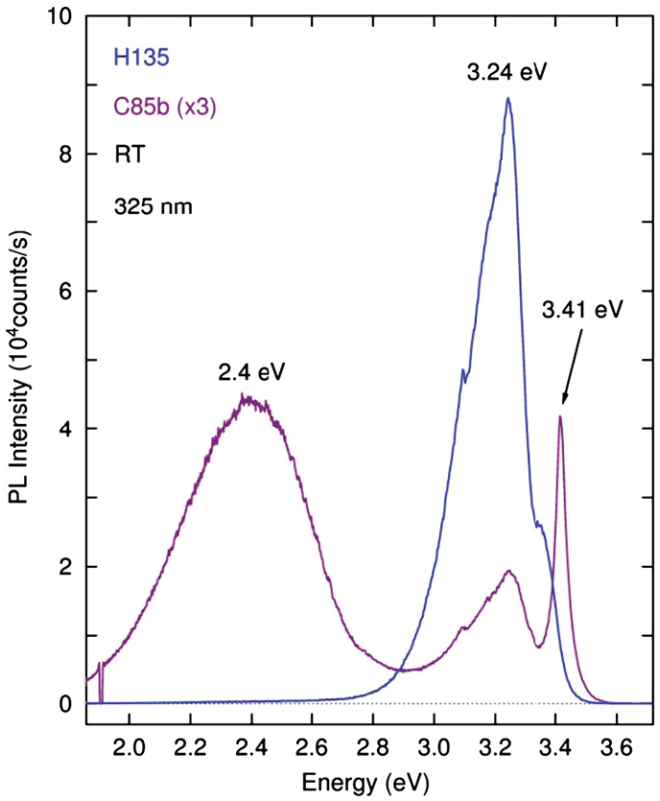

Fig. 6. Room temperature PL spectrum of two crystals. The low temperature PL spectra of the sample with dominant room temperature DAP emission band is also represented in Figs. 3 and 4, where it is evident the prevailing recombination process involving acceptors.

shows only an intense 3.24 eV band, indicating that the recombination is dominated by F–B process. Similar RT spectral trend has been observed in PL studies of thin films doped with Mg impurities. The lack of the NBE emission and yellow-green bands in the PL spectra suggests that the Fermi level moved deeper into the forbidden gap toward the acceptor energy level. Note that, the low resolution LT PL spectrum of the Sample H135, represented in Fig. 3 shows a dominant DAP pair band with weak yellow band and reduced NBE emission band contributions. In addition, the high resolution LT PL spectrum of this sample clearly shows that the dominant recombination at the NBE spectral region is related to the annihilation of the exciton bound to neutral acceptors. Similar spectra have been observed in homoepitaxial films doped with Mg, which show p-type conductivity at RT [23]. These observations suggest that samples with n-type or p-type conductivity may be generated by this growth method, which has low background impurity concentrations, as supported by preliminary SIMS data, by controlling the growth conditions. Additional experiments, such SIMS and Hall measurements among others, will be carried out when larger samples become available to identify the chemical nature and concentration of the dominant acceptor.

5. Conclusion

Raman scattering, supported by previously reported XRD rocking curve measurements, demonstrated that near atmospheric pressure solution growth method produces basal plane self-nucleated crystals of high crystalline quality. Records of small first order phonon FWHM were observed, which are consistent with the lower values observed for the XRD curves. Differently from ammonothermal growth and high nitrogen pressure solution growth, the proposed growth method yield crystals with low background free carrier concentration, as supported by room and low temperature PL experiments and by preliminary SIMS data. The similarity of the LT and RT luminescence spectra of these platelets with the spectra of Mg doped epitaxial films suggest that partially or fully compensated samples, or sample with small excess of free holes could be produced under slightly different growth conditions. Additional experiments with larger samples are planned in order to measure the concentration and to identify the chemical nature of the background impurities, and to verify the dominant carrier type.

References

[1] I. Akasaki, in: Proceedings of the International Workshop on Nitride Semiconductors, IPAP Conference Series 1, 2000, p. 1.
[2] S. Yoshida, S. Mizawa, S. Gonda, Appl. Phys. Lett. 42 (1983) 427.
[3] H. Amano, N. Sawaki, I. Akasaki, T. Toyoda, Appl. Phys. Lett. 48 (1986) 353.
[4] S. Nakamura, Jpn. J. Appl. Phys. 31 (1992) L139.
[5] H.P. Maruska, J.J. Tietjen, Appl. Phys. Lett. 15 (1969) 327.
[6] M.K. Kelly, R.P. Vaudo, V.M. Phanse, L. Gögens, O. Ambacher, M. Stutzmann, Jpn. J. Appl. Phys. 38 (1999) L217.
[7] S.S. Park, Il-W. Park, S.H. Choh, Jpn. J. Appl. Phys. 38 (1999) L217.
[8] T. Yoshida, Y. Oshima, T. Eri, K. Ikeda, S. Yamamoto, K. Watanabe, M. Shibata, T. Mishima, J. Cryst. Growth 310 (2008) 5.
[9] J.A. Freitas Jr., W.J. Moore, B.V. Shanabrook, G.C.B. Braga, S.K. Lee, S.S. Park, J.Y. Han, D.D. Koleske, J. Cryst. Growth 246 (2002) 307.
[10] M. Murthy, J.A. Freitas Jr., J.-H. Kim, E.R. Glaser, D. Storm, J. Cryst. Growth 305 (2007) 393.
[11] K. Motoki, T. Okahisa, R. Hirota, S. Nakahata, K. Uematsu, N. Matsumoto, J. Cryst. Growth 305 (2007) 377.
[12] D. Hanser, L. Liu, E.A. Preble, K. Udwary, T. Paskova, K.R. Evans, J. Cryst. Growth 310 (2008) 3953.
[13] C. Wetzel, M. Zhu, J. Senawiratne, T. Detchprohm, P.D. Persans, L. Liu, E.A. Preble, D. Hanser, J. Cryst. Growth 310 (2008) 3987.
[14] R.M. Farrel, D.F. Feezell, M.C. Schmidt, D.A. Haeger, K.M. Kelchner, K. Iso, H. Yamada, M. Saito, K. Fujito, D.A. Cohen, J.S. Speck, S.P. DenBaars, S. Nakamura, Jpn. J. Appl. Phys. 46 (2007) L761.
[15] R. Dwilinski, R. Doradzinski, J. Garczynski, L.P. Sierzputowski, A. Puchalski, Y. Kanbara, K. Yagi, H. Minakuchi, H. Hayashi, J. Cryst. Growth 311 (2009) 3015;
R. Dwilinski, R. Doradzinski, J. Garczynski, L.P. Sierzputowski, M. Zajac, M. Rudzinski, J. Cryst. Growth 311 (2009) 3058.
[16] R. Kucharski, M. Rudzinski, M. Zajac, R. Doradzinski, J. Garczynski, L. Sierzputowski, R. Kudrawiec, J. Serafinczuk, W. Strupinski, R. Dwilinski, Appl. Phys. Lett. 95 (2009) 131119.
[17] F. Kawamura, M. Morishita, M. Tanpo, N. Imade, M. Yoshimura, Y. Kitaoka, Y. Mori, T. Sasaki, J. Cryst. Growth 310 (2008) 3946.
[18] B.N. Feigelson, R.M. Frazier, M. Gowda, J.A. Freitas Jr., M. Fatemi, M.A. Mastro, J.G. Tischler, J. Cryst. Growth 310 (2008) 3934.
[19] L. Bergman, D.A. Alexson, P.L. Murphy, R.J. Nemanich, M. Dutta, M.A. Stroscio, C. Balkas, H. Shin, R.F. Davis, Phys. Rev. B 59 (20) (1999) 12977–12982.
[20] R. Stepniewski, A. Wysmolek, M. Potemski, K. Pakula, J.M. Baranowski, I. Grzegory, S. Porowski, G. Martinez, P. Wider, Phys. Rev. Lett. 91 (2003) 226404.
[21] M.A. Reshchikov, H. Morkoç, J. Appl. Phys. 97 (2005) 061301.
[22] M. Gouda, J.A. Freitas Jr., R.M. Frazier, B.N. Feigelson, M.V. Rao, J. Cryst. Growth 310 (2008) 3941.
[23] E.R. Glaser, M. Murphy, J.A. Freitas Jr., D.F. Storm, L. Zhou, D.J. Smith, Physica B 401 (2007) 327.
[24] B. Monemar, P.P. Paskova, G. Pozina, C. Hemmingsson, J.P. Bergman, T. Kawashima, H. Ammano, I. Akasaki, T. Paskova, S. Fogge, D. Hommel, Usui, Phys. Rev. Lett. 102 (2009) 235501.
[25] E.R. Glaser, J.A. Freitas Jr., B.V. Shanabrook, D.D. Koleske, S.K. Lee, S.S. Park, J.Y. Han, Phys. Rev. B 68 (2003) 195201.
[26] J.A. Freitas Jr., W.J. Moore, B.V. Shanabrook, G.C.B. Braga, S.K. Lee, S.S. Park, J.Y. Han, Phys. Rev. B 66 (2002) 233311.
[27] R. Dwilinski, R. Doradzinski, J. Garczynski, L.P. Sierzputowski, M. Zajac, M. Rudzinski, J. Cryst. Growth 311 (2009) 3062.
[28] P. Perlin, T. Suski, M. Leszczynski, T. Teisseyre, Optoelectronic properties of semiconductors and supperlattice, in: S.J. Pearton (Ed.), GaN and Related Materials, vol. 2, Gordon and Breach, London, 2007, p. 315.
[29] R. Dwilinski, R. Doradzinski, J. Garczynski, L.P. Sierzputowski, J.M. Baranowski, M. Kaminska, Mater. Sci. Eng. B 50 (1997) 46.
[30] B.J. Skromme, K. Palle, C.D. Poweleit, H. Yamane, M. Aoki, F.J. DiSalvo, J. Cryst. Growth 246 (2002) 299.
[31] J.A. Freitas Jr., K. Doverspike, A.E. Wickenden, Mater. Res. Soc. 395 (1996) 485.
[32] R. Armitage, Q. Yang, E.R. Weber, J. Appl. Phys. 97 (2005) 073524.
[33] A.E. Wickenden, D.D. Koleske, R.L. Henry, R.J. Gorman, M.E. Twigg, M. Fatemi, J.A. Freitas Jr., W.J. Moore, J. Electron. Mater. 29 (21) (2000) R114.